LA-UR- 93-2276

Title: MEASUREMENT AND ANALYSIS OF THREE 1.5-GPA SHOCK-WAVE PROFILES IN COPPER

Author(s): Richard H. Warnes, M-7

Davis L. Tonks, X-4
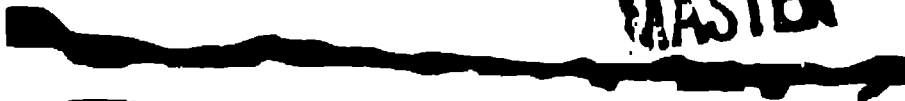
MASTER

Los Alamos
NATIONAL LABORATORY

MEASUREMENT AND ANALYSIS OF THREE 1.5-GPA SHOCK-WAVE PROFILES IN COPPER

Richard H. Warnes and Davis L. Tonks
Los Alamos National Laboratory
Los Alamos, NM 87545 USA

Three wave-profile experiments were performed on OFE fully annealed (600 °C for one hour) copper us ing a 101.6-mm-diam gas gun at impact velocities of 86 m/s. A symmetric impact produced a 1.5-GPa shock wave in the target. A sapphire window was bonded to the front (non-impact) face of the target, and a four-detector push-pull velocity interferometer (VISAR) measured the velocity of the cop per/sapphire interface. The impactor thickness (4 mm) was the same in all experiments; the target thicknesses were 10, 20, and 30 mm. The stresses and strains, including the deviatoric stresses and strains, have been extracted from these data using a quasi-Lagrangian analysis. (The waves are not steady.) The use of three separate shots in Lagrangian analysis yields only approximate results for the deviatoric stresses; but the results for the normal stresses, and for the strains, are fairly accurate. Even though the strain rates fall in the Hopkinson bar regime, the mechanism of dislocation motion ap pears to be dislocation drag, as is the case for stronger shock waves in Cu.

INTRODUCTION

The three experiments presented here are part of a series of experiments to measure and model the elastic plastic response of OFE fully annealed copper subjected to shock and reshock and shock and release loading at initial pres sures of 1.5 and 3 GPa. Some of the 3 GPa ex periments and analyses have already been re ported [1]. This paper presents the very lowest pressure experiments and analyses.

EXPERIMENTS

A 101.6-mm diam gas gun was used to pro duce a symmetric impact in OFE copper at an impact velocity of about 86 m/s. The copper in both the impactor and the target was fully an nealed (600°C for one hour). A single crystal sapphire window [2] was bonded to the front (non impact) face of the copper target.

The impactor velocity was measured with an array of electrical contact pins recording on digi tizers with a resolution of 5 ns. The velocity of the target/sapphire interface was measured with a four detector push pull VISAR [3] recording on digitizing oscilloscopes sampling at either 1 or 2 gigasamples/s.
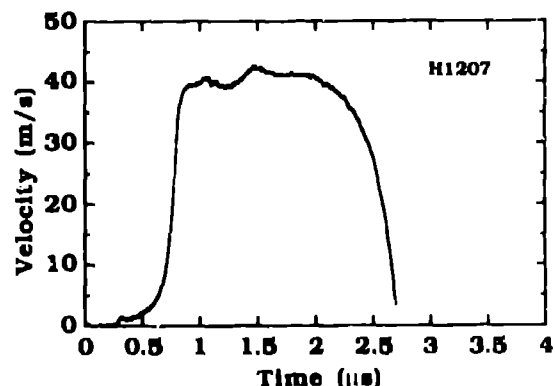

Figure 1. Experiment H1207; 10 mm target. The velocity is at the Cu/sapphire interface.

In these three low stress, low strain rate ex periments the impactor thickness was 4 mm, and the target thicknesses were 10 mm, 20 mm, and 30 mm. Details of the experiments are given in Tables 1 and 2. The wave profiles at the target/sapphire window interfaces are plotted in Figs. 1-3.

Table 1. Dimensions of components in the experiments.

Experiment No.	Impactor Thickness (mm)	Impactor Diam (mm)	Target Thickness (mm)	Target Diam (mm)	Sapphire Window Thickness (mm)	Sapphire Window Diam (mm)
H1207	3.988	50.957	9.970	54.953	25.0	50.0
H1208	3.988	50.944	19.952	54.953	25.0	50.0
H1230	3.988	50.944	29.972	54.940	25.0	50.0

Table 2. Impact velocities and VISAR setup.

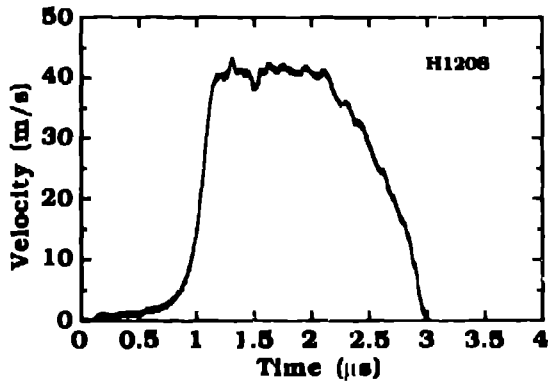| Experiment No.	Impactor Velocity (m/s)	Impactor Tilt (mrad)	Fringe Constant (m/s)
H1207	85.7 ±0.1	0.85	39.07
H1208	85.2 ±0.3	0.66	39.07
H1230	86.2 ±0.1	1.21	39.07

Figure 2. Experiment H1208; 20-mm target. The velocity is at the Cu/sapphire interface.
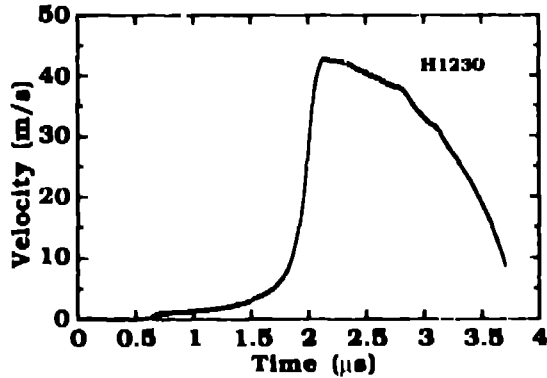

Figure 3. Experiment H1230; 30 mm target. The velocity is at the Cu/sapphire interface.

THEORETICAL ANALYSIS

The particle velocity data were smoothed by local least squares fitting to eliminate local ringing that changed the sign of the acceleration This resulted in no drastic changes to the data.

Theoretically, Lagrangian analysis requires progressive snapshots of the same wave. The

data available here, however, are from three different experiments with three different sample thicknesses. (See Table 1.) Shot-to-shot variations cloud the straightforward application of the technique to these data. For example, as seen in Figs. 1-3, experiment H1230 has a somewhat larger peak velocity than the others. In order to apply the Lagrangian method, these variations must be eliminated in some fashion. Therefore, the profiles for experiments H1207 and H1208 were scaled in velocity to make their peak velocities identical to that of shot H1230. (The adjustments were minor, less than eight percent.) The method of analysis used here consists of a Lagrangian analysis together with this and other methods of eliminating shot-to-shot variations (to be described shortly). It will be called a pseudo-Lagrangian analysis.

To estimate the extent of the error, each wave was analyzed using the steady wave analysis of Wallace [4] and the results were compared to that of the pseudo-Lagrangian method used here. The steady wave results are surely not correct, but provide some sort of bound on the correct result. As seen in Figs. 4-7, the results from both analyses compared fairly closely for all quantities except the deviatoric stress, which is the quantity most sensitive to error. Nevertheless, the two versions of the deviatoric stress, Fig. 5, are similar, differing at most by about 30%.
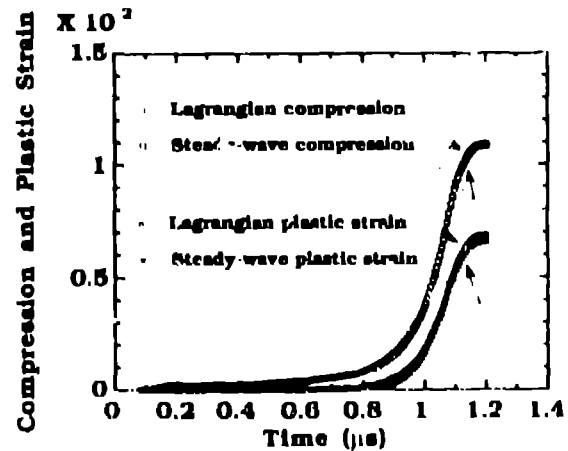

Figure 4. Calculated compression and plastic strains versus time for the H1208 gauge position.

A 3% elastic impedance correction was applied to the measured interface velocity to esti

mate the in situ Cu particle velocity without the presence of the sapphire. For a correction this small, the elastic theory is adequate, [5].

The Lagrangian method of paths was used, [7]. Each profile was divided into three monotonic parts separated by the peak of the first rise, the following dip, and the top of the plastic wave. Points with the same relative velocity in corresponding parts in the three profiles were connected to form paths.

The equations used for the pseudo-Lagrangian analysis are

$$\sigma(t) = -\rho_0 \int \left(\frac{\partial u}{\partial t} \right)_h dh \Big|_t \qquad (1)$$

and

$$\epsilon = -\int \left(\frac{\partial u}{\partial h} \right)_t dt \Big|_h . \qquad (2)$$

where u is the particle velocity, σ is the normal stress defined positive in compression, ϵ is the compression or volumetric strain, h is the Lagrangian position, ρ_0 is the initial density, and t is the time. The normal stress and compression were found at the sample thickness (20 mm) corresponding to shot 111208 using these formulas. Eq. (1) was integrated along a line of constant time in the h t plane inward from an undisturbed position in front of the shock wave. Eq. (2) was integrated along a line of constant h corresponding to the 111208 sample thickness. The 111208 position is in the center of the data and, thus, extrapolations there are minimized.

Once σ and ϵ were obtained, the thermoelastic equations of Wallace [4] were used to obtain the deviatoric stress and plastic strains. The material parameters used are given in [5,6].

The steady wave procedure used to obtain the steady wave results are also described in these references. In the calculations here, the rise to the first peak was assumed elastic and the velocity of point "c" used in the analysis [4] was taken to be 10 m/s.

The absolute timing measurements of the transit time for the three profiles proved to be too inaccurate to obtain physically reasonable results; negative deviatoric stresses were obtained. Using the points of first motion to aid in aligning the three records, in some also led to negative deviatoric stresses. To set the relative timing of the three profiles, the peaks of the first rise were taken to have traversed the sample

thicknesses at the longitudinal sound velocity. This assumption, together with the velocity versus time record for each profile, established the timing for all profile points.
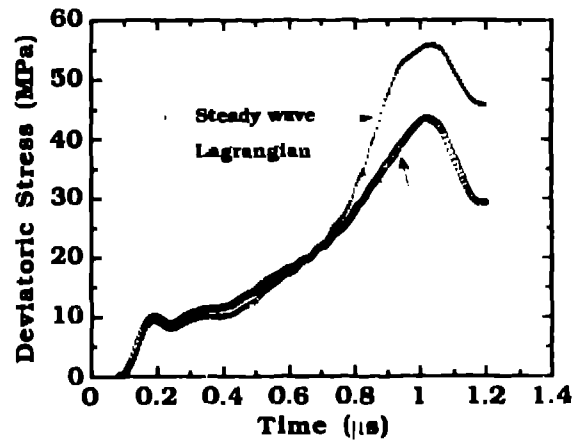

Figure 5. Calculated deviatoric stress versus time for the 111208 gauge position.
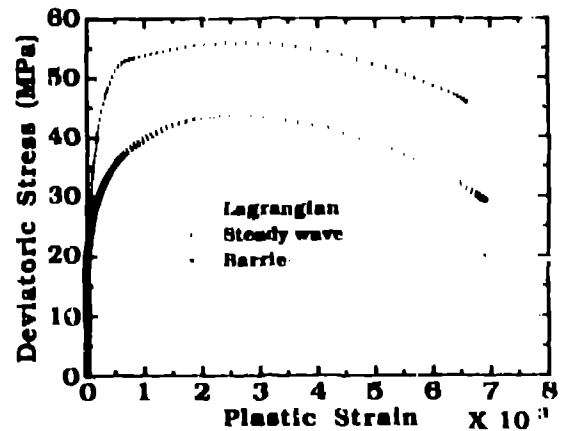

Figure 6. Calculated deviatoric stress versus plastic strain for the 111208 gauge position. The X is a calculated value for the internal barrier strength at the top of the shock wave.

Both linear and quadratic fitting of the data were tried. Both gave about the same results for the stresses and strains at the 111208 target thickness. The calculated peak deviatoric stress, however, was about 10% lower for the quadratic fit than for the linear fit. For the thicknesses

corresponding to the other two experiments the quadratic fit gave regions of negative deviatoric stress. These results are not shown here. Since the linear fit did not produce this problem, only the linear results are given here. One would think that the quadratic fit would give better results because it was based on all of the data. The reason it did not may be due to the shot to shot variations.

An additional restriction is that only data from shots 111208 and 111230 were used in the linear fit. Using data from shots 111207 and 111208 in the linear fit also produced negative deviatoric stresses.
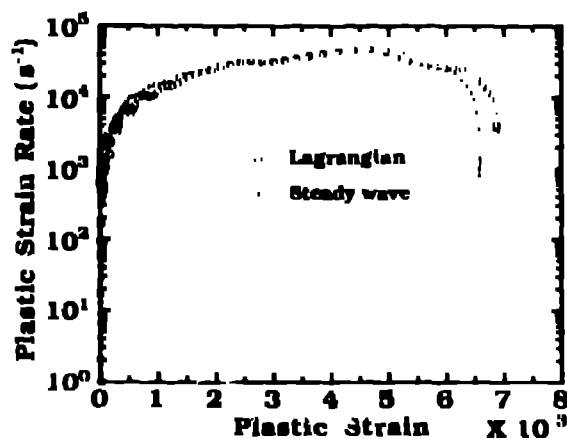

Figure 7. Calculated plastic strain rate versus plastic strain for the 111208 gauge position.

We note that the deviatoric stress used here is: $r \left(\frac{1}{2} \right) (r_{xx} - r_{yy})$, where r_{xx} and r_{yy} are the stresses along, and normal to, the shock direction, respectively.

The curves of the deviatoric stress versus plastic strain, Fig. 6, and of the strain rate versus plastic strain, Fig. 7, closely resemble those for stronger Cu shock wave profiles that are dominated by dislocation drag [1]. The very last rise in plastic strain rate with plastic strain and the peaking of the deviatoric stress about midway in plastic strain are typical of shock wave dislocation drag processes in which the initial stress loading is higher than any initial barriers and faster than any buildup of internal work hardening. Hence, the mechanism of plastic flow here is probably influenced by dislocation drag also.

Evidence for this was obtained by calculating, for the end of the shock path of Fig. 6, the mechanical threshold stress using the model of [8]. Because of the small strains involved, the results of this model should be considered fairly rough, accurate to, say, 40%. The resulting value of 20 MPa for the mechanical threshold stress should be compared with the final deviatoric stress of Fig. 6. Due to the uncertainties involved, these two values are roughly the same. As can be seen, after the first rise the deviatoric stresses of the shock path lie above this value, which is an upper bound for the evolving threshold stress, indicating that the dislocations are being driven by stresses greater than the opposition of internal barriers. Hence, even though the strain rates here fall in the range of Hopkinson bar data, which is dominated by thermally activated dislocation motion, the stress loading here is higher than internal barriers and so abrupt that dislocation drag is the mechanism of dislocation motion.

ACKNOWLEDGMENTS

REFERENCES

[1] R. H. Warnes and D. L. Tonks, "Measurement and Analysis of 3 GPa Shock Wave Profiles in Annealed OFE Copper," in Proceedings of the APS Topical Conference on Shock Compression of Condensed Matter, 1989, pp. 329-332.

[2] L. M. Barker and R. E. Hollenbach, J. Appl. Phys 41, pp. 4208-4226 (1970).

[3] W. F. Hemsing, Rev. Sci. Instrum. 50(1), pp. 73-78 (1979).

[4] D. C. Wallace, Phys. Rev. B 22, pp 1477-1486 and 1487-1494 (1980).

[5] D. L. Tonks, J. Appl. Phys. 66, pp.1951-1960 (1989).

[6] D. L. Tonks, "The DataShoP, A Database of Weak Shock Constitutive Data," Los Alamos National Laboratory Report LA 12068 MS, (1991).

[7] L. Seaman, J. Appl. Phys. 45, p. 4303 (1974).

[8] J. N. Johnson and D. L. Tonks, "Dynamic Plasticity in Transition from Thermal Activation to Viscous Drag," in Proceedings of the APS Topical Conference on Shock Compression of Condensed Matter, 1991, pp. 371-378.

DISCLAIMER